Real-time holographic information processing at near infrared using ruthenium-doped bismuth sillenite crystals

Shiuan Huei Lin[a,*], Vera Marinova[b,c], Ren Chung Liu[c] and Ken Y. Hsu[c]
[a]Department of Electrophysics, National Chiao Tung University, HsinChu, Taiwan;
[b]Institute of Optical Materials and Technologies, Bulgarian Academy of Science, Sofia 1113, Bulgaria;
[c]Institute of Electro-Optical Engineering & Department of Photonics, National Chiao Tung University, HsinChu, Taiwan

ABSTRACT

In this paper, we report our investigations on real-time holographic recoding at 1064 nm in Ru-doped bismuth sillenite crystal with a green gating light at 532 nm. By using gating light significant improvement of the response time to 80 ms is achieved and the prolonged read-out process of the recorded hologram is observed. We also demonstrate quasi-permanent holographic recording of image with fast speed in Ru-doped BSO crystal using two-wavelength recording.

Keywords: Holography, photorefractive crystal, near infrared photorefractive effect, two-wavelength recording

1. INTRODUCTION

Crystals of the form $Bi_{12}MO_{20}$ (M representing Si, Ti, or Ge), termed sillenites, and are known to be promising candidates for use in dynamic holographic applications due to their particularly rapid and highly sensitive photorefractivity [1]. Among them, $Bi_{12}SiO_{20}$ (hereinafter named BSO), is most popular in practical applications because of its easier growth processing and higher signal-to-noise ratio as well as its holographic sensitivity in the red spectral range. In addition, sillenite crystals have a wide bandgap, in which the intrinsic defects of the crystal structure act as an attractive matrix for doping elements (extrinsic defects), and thus transition metals and rare-earth elements can easily be incorporated into the crystal structure to create new photorefractive trap centers. Both of intrinsic and impurity defects can act as photochromic and photorefractive traps such that the doped sillenite crystals have easily multiple donor/acceptor levels in the band structure. It is known in photorefractive physics that these multiple levels will participate in the charge generation and transportation mechanism, and then modify crystal properties to provide new photorefractive properties. In past years a lot of research has been conducted and several doping elements has been proposed and introduced into the sillenite structure for tailoring their properties especially for optical information processing at real-time scale [2]. Recently, special attention is focused on near infrared (NIR) sensitivity improvement [3-5], which is of essential technological interest since it allows utilization of cheap diode lasers in photorefractive devices development for optical fiber communication as well as of particular importance for non-destructive biological object testing.

We reported that Ruthenium (Ru) is an appropriate dopant, which significantly improves the NIR sensitivity of $Bi_{12}TiO_{20}$ (BTO) [6,7]. Ramaz et al. [8] observed very high photorefractive gain of Ru-doped $Bi_{12}SiO_{20}$ (BSO) in a diffusion regime using 647 nm. These results show that addition of Ru provides prospective features for improving NIR photorefractivity in sillenite crystals. In this paper, we report on the response time and sensitivity enhancement of BSO at near infrared spectral range (at 1064 nm) with appropriate amount of Ru-doping and pre-exposure with green light (532 nm). Additionally, prolonged read-out process of a hologram recorded with simultaneous exposure to green light is observed. We demonstrate quasi-permanent holographic recording of image with fast updating speed (~ few seconds) in Ru-doped BSO crystal. The results show that this crystal is promising photorefractive material for real-time holographic information processing. We then propose a theoretical model based on two photorefractive traps in the band structure for analyzing recording dynamics. From the analyses, it can be conjectured that the fundamental issue to achieve non-volatile photorefractivity in Ru-doped BSO crystals is to have small enough (even zero) thermal generation rate constant of deep trap.

*lin@mail.nctu.edu.tw; phone 886 3 5712121ext 56173; fax 886 3 5725230

Photonic Fiber and Crystal Devices: Advances in Materials and Innovations in Device Applications V, edited by Shizhuo Yin, Ruyan Guo, Proc. of SPIE Vol. 8120, 81200I · © 2011 SPIE · CCC code: 0277-786X/11/$18 · doi: 10.1117/12.891801

2. EXPERIMENTS

2.1. Crystal Growth

Ru-doped BSO crystals were grown from stoichiometric solutions by the Czochralski method [9]. The starting products Bi_2O_3 and SiO_2, with purity 99.999%, were introduced in a weight ratio of 11:1. Doping element, Ru was added to the melt solution. The Ru concentration (up to $6.1x10^{18}$ cm^{-3} in the grown crystals) was determined by atomic absorption spectrometry. Double side optically polished parallel crystal plate with a thickness of 0.45 mm was used for optical absorption measurements at visible and NIR range. For holographic experiments, cube with rectangular dimensions 10.3 x 11.4 x 6.4 mm along (110), (1$\bar{1}$0) and (001) crystallographic directions was prepared.

2.2. Optical experiments

Optical absorbance spectra were measured on double polished plates in the wavelength range 350-2000 nm using Shimadzu spectrophotometer (model UV 3600). The transmission spectrum of the crystal plate was examined with two extreme states of the crystal: bleached state (thermodynamically stable) and colored state (thermodynamically metastable). To reach colored state, the grown Ru-doped BSO crystal was illuminated by a 532 nm cw light coming from Verdi laser source (intensity ~250mW/cm^2) for 5 min irradiation. After measurement, the sample was annealed to reach the bleached state by heating in an oven to over 180°C for an hour.

In the holographic experiments, diode-pumped laser operating at 1064 nm was used to write gratings in a two-wave beam interference set-up in transmission geometry. The optical setup is shown in Fig.1. The intensity of each recoding beam was about 150 mW/cm^2 and the writing angle between two beams is 30° outside the crystal. The grating was monitored at real time with low power third beam, coming from the same laser source. The diffracted light was measured with a Si detector located behind the crystal. Another 532 nm cw light coming from Verdi laser source (adjustable intensity) was used for illumination to perform two-wavelength recording. The sample was thermally annealed before the experiments. For image recording/reconstruction experiment the above described set-up was slightly modified. The signal beam carried the magnified image of the mask, which is detected by the CCD camera (640 x 480 pixels) and the image is reconstructed by the reference beam.

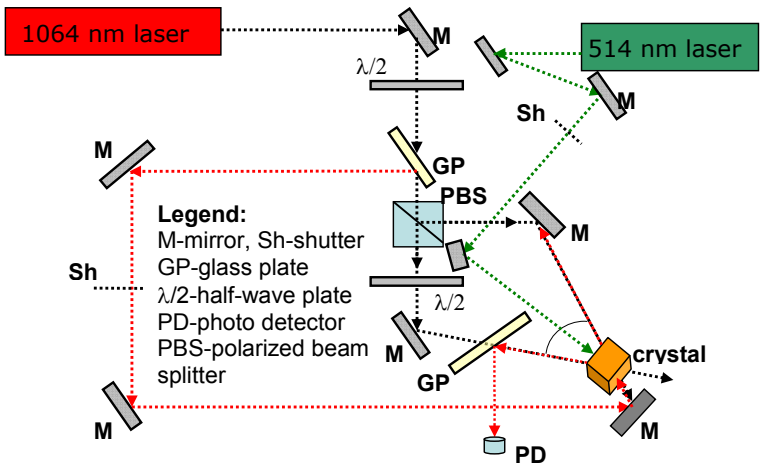

Figure 1. Optical setup for holographic recording in Ru-doped BSO crystal with excitation using green light

3. EXPERIMENTAL RESULTS AND DISCUSSIONS

3.1. Absorption spectrum

Figure 2 shows the absorption spectra of Ru-doped BSO crystals. For comparison, the spectrum of non-doped BSO is also presented. The absorption shoulder in non-doped BSO is located at 500 nm, which provide an intrinsic

photorefractive centers in green spectral region. The absorption shoulder is shifted from green to red (even NIR) spectral range by doping Ru in BSO. It indicates Ru dopants introduce shallower traps, which give possibility for recording hologram in NIR spectral range. Additionally, after exposure to the green light to reach colored state, a broad near infrared absorption peak (with rather low intensity) is detected with a maximum around 1320 nm. This strong change of absorption spectrum between annealed and colored states shows the shallower levels induced by addition of Ru dopants also play a role of photochromic center. Operating together with the above intrinsic traps in green range, the photorefractive properties can be manipulated with a green light gating. It suggests further possibility of holographic recording with two-wavelength recording scheme: NIR wavelength (λ=1064 nm) for recording and green wavelength for gating (λ=532 nm) in our Ru-doped BSO crystal.

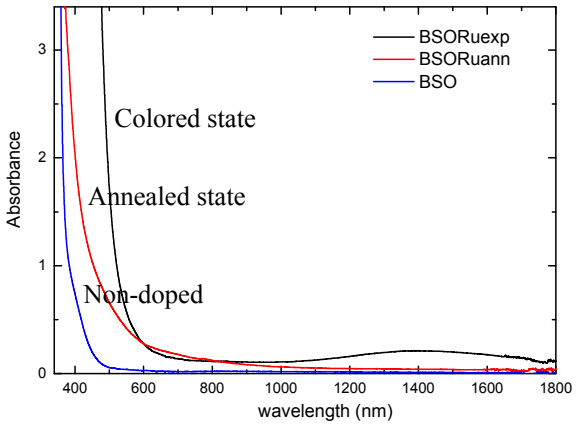

Figure 2. Absorption spectra of non- and Ru-doped BSO crystals at bleached state (exp.) and colored state (ann.).

3.2. Holographic recording

Figure 3 shows comparison between recording and read-out dynamics processes of Ru-doped BSO crystal at 1064 nm without and after pre-exposure with gating light of 532 nm (220 mW/cm^2 for 5 min.). As it seen, without pre-exposure the sample does not reach the saturation state until 20 s (complete process presented as inset graph in Figure 3). Once the crystal is exposed to green light to reach the colored state, significant improvement of the recording speed is detected and the writing kinetics shows very fast growth with response time of 80 ms. The fast decay kinetics of the hologram during read-out process (after 2 s) using uniform reference beam is also observed. The writing process seems to be fitted well with single exponential curve. It indicates that the shallow traps play a major role during holographic recording for the case of pre-exposure. However, optical excitation energy for deep intrinsic traps is roughly located close to 2 eV (green light). It can be used to pump photocarriers in the intrinsic deep levels to the main photorefractive level via conduction band in BSO structure. Thus, with helping of pre-exposure to green light, the shallow traps contain more carriers which are sensitive to 1064 nm laser and participate the photorefractive process to enhance recording speed. This technique, using gating light to pump optically the electrons is recognized method to enhance the beam coupling gain [10] as well as to improve the sensitivity and achieve infrared recording in non-doped sillenites [3]. In addition, it is seen that the prolonged read-out process after 2.5 s in the Ru-doped BSO is observed, although the diffracted signal is rather weak. It suggests that photo-excited charge carriers are not directly re-trapped by shallow centers, but it is very possible small amount of carriers is also captured by deep centers. The deep level is located few electron volts away from the CB (or the VB) such that it can't be excited by 1064 nm laser. The trapped charge carriers can only be re-excited by thermal excitation without green light. Thus, we anticipate that the life time of hologram at 1064 nm can be further extended with appropriate illumination to green gating light. Next, we show the results for recording at 1064 nm with 532 nm gating simultaneously.

Figure 4 shows comparison between recording and read-out dynamics processes of Ru-doped BSO crystal at 1064 nm without and with gating light of 532 nm simultaneously. As it seen, both dynamics of the recording and read-out processes are quite complicated when two wavelengths illuminated the crystal. The recording process starts with fast growth during the first few tens ms, followed by decrease of the diffracted beam intensity after prolonged time of the

recording. The read-out process (after 3.2 s) starts with fast decay in the beginning, followed by slow decrease of the diffracted beam intensity as the intensity of gating is weak (< 100mW/cm^2). The diffracted signal even becomes oscillation as the intensity increases and the grating persists for longer life time. In the past, this observed transient character was assigned to the competition of simultaneous electron-hole gratings [10]. However, we will show theoretically in section 4 that the origin of such response can be attributed to the above mentioned two different trap centers with the same type of photocarrier, each of them creating own grating with different signs, amplitude and response time due to the their different optical properties.

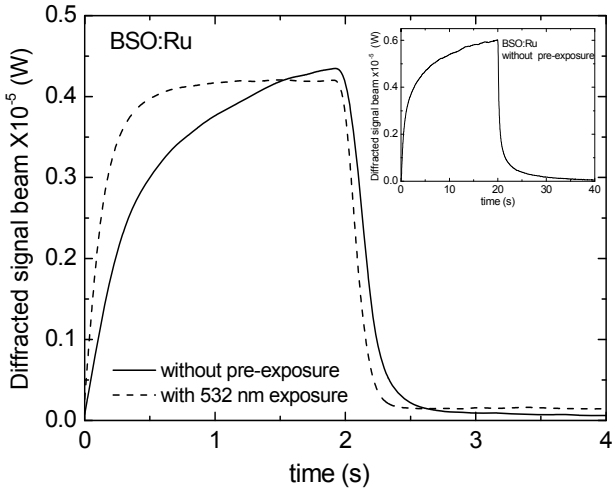

Figure 3. Comparison of recording and read-out process of BSO:Ru crystal at 1064 nm: solid line - without any preliminary treatment, dot line - after green light pre-exposure (220 mW/cm^2). Inset graph: BSO:Ru sample reaches saturation state.

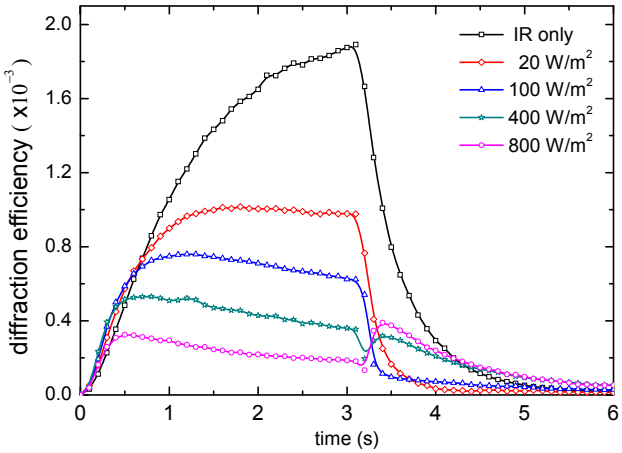

Figure 4. Holographic dynamics of the recording and read-out processes of BSO:Ru crystal: using λ=1064 nm for recording and probing and simultaneous gating by λ=532 nm with different intensity during the recording. The read-out process only by λ=1064 nm.

3.3. Quasi-permanent image recording

In addition to show the NIR photorefractivity of Ru-doped BSO, image recording/reconstruction experiments were conducted. Figure 5 shows the time evolution of the reconstructed images, taken by CCD camera. There were two holograms recorded in the same location with two different conditions. One was the Fourier hologram of a letter “B”

image. It was recorded using 1064-nm beams with gating illumination of 532 nm simultaneously. The other was that of a resolution chart image, which was recorded at single wavelength of 1064 nm with pre-exposure to 532 nm laser. As it seen, there are two images reconstructed simultaneously in the beginning. The reconstructed image of resolution chart fades away gradually and almost disappears after 20 s. At the same time scale, the reconstructed image of letter "B" still remains. To the best of our knowledge this is the first demonstration in sillenite crystals, which shows an extended lifetime of holographic grating at near infrared and at room temperature using a gating light. The estimation of lifetime of the grating as well as the optimizations of experimental and material conditions to achieve nonvolatile memory are underway.

(a) 0s (b) 5s (c) 10s (d) 20s

Figure 5. Time evolution of the image reconstruction in Ru-doped BSO without and with gating illumination.

4. THEORETICAL CONSIDERATION

4.1 Modeling

Temporal responses of holographic recording and read-out behavior in experiments can be analyzed by using theoretic modeling of two-wavelength photorefractive grating recording [11]. Since the absorption spectral measurement suggests existence of multiple photorefractive traps in our Ru-doped BSO, we assume there are two kinds of trap centers. One is shallow so that the carriers can be excited by the laser with longer wavelength (λ=1064 nm). The other is deep in which laser with shorter wavelength (λ=532 nm) is efficient to excite carriers. Thus, the dynamic behavior of photorefractive effect in this crystal can be described by the following set of nonlinear coupled equations and appropriate recording scheme, which is modified Kukhtarev band transport model [12] by adding one more electron changing rate equation (e.g. Eq.(2)) for another trap center:

$$\frac{\partial N_1^+}{\partial t} = (N_1 - N_1^+)(s_{11} I_1 + \beta_1) - r_1 n N_1^+ \tag{1}$$

$$\frac{\partial N_2^+}{\partial t} = (N_2 - N_2^+)(s_{21} I_1 + s_{22} I_2 + \beta_2) - r_2 n N_2^+ \tag{2}$$

$$\frac{\partial n}{\partial t} = \frac{\partial N_1^+}{\partial t} + \frac{\partial N_2^+}{\partial t} + \frac{1}{e}\frac{\partial J}{\partial z} \tag{3}$$

$$J = e\mu n E + \mu k_B T \frac{\partial n}{\partial z} \tag{4}$$

$$\varepsilon \frac{\partial E}{\partial z} = e(N_1^+ + N_2^+ - n - N_A) \tag{5}$$

where the physical meanings and values of terms and crystal parameters are listed in Table 1. Following the standard procedure of linearization, which is legitimate for small modulation depth, we assume the following forms for various physical quantities:

$$N_1^+ = N_{10}^+ + N_{11}^+ e^{-iKz} \tag{6}$$

$$N_2^+ = N_{20}^+ + N_{21}^+ e^{-iKz} \tag{7}$$

$$n = n_0 + n_1 e^{-iKz} \tag{8}$$

$$J = J_0 + J_1 e^{-iKz} \tag{9}$$

$$E = E_0 + E_{SC} e^{-iKz} \tag{10}$$

and then solve the coupled equations (6)-(10) for the zero- and first-order terms with intensities of the exciting and recording lasers given by two cases:

(1). pre-illumination with green gating

$$I_1 = \begin{cases} I_{10}, \text{ before recording stage} \\ 0, \text{at recording and red - out stage} \end{cases} \tag{11}$$

$$I_2 = \begin{cases} I_{20}(1 + me^{-iKz}), \text{ at recording stage} \\ I_{20}, \text{at read - out stage} \end{cases} \tag{12}$$

(2). illumination with green gating and recording hologram simultaneously

$$I_1 = \begin{cases} I_{10}, \text{ at recording stage} \\ 0, \text{at read - out stage} \end{cases} \tag{13}$$

$$I_2 = \begin{cases} I_{20}(1 + me^{-iKz}), \text{ at recording stage} \\ I_{20}, \text{at read - out stage} \end{cases} \tag{14}$$

where I_1 is the intensity of exciting laser with shorter wavelength, I_2 is the intensity distribution of the interference fringe formed by two recording laser beams with longer wavelength, and m is the modulation depth. In these terms, the zero-order terms N_{10}^+, N_{20}^+ and n change very rapidly towards their steady-state value, compared to the rate at which the first-order terms N_{11}^+, N_{21}^+ and n_1. Therefore, we can solve the set of equations (1)-(5) by firstly calculating the zero-order terms and then using these values to solve for the temporal evolution of E_{SC} at both recording and erasure stages by use of different crystal parameters. Because of the electro-optical effect in photorefractive crystal, the change of the refractive index grating during holographic recording and erasure is proportional to the temporal evolution of E_{SC}. This theoretical consideration can be used to explain the above holographic experimental results. During calculation, we found that one qualitative result needs to be noted here. By inducing the gating light during holographic recording, two complimentary space charge gratings result from two traps are recorded in these photorefractive crystals. It is usually considered as the reason why the non-volatile photorefractive hologram can be recorded the $LiNbO_3$ crystals [11].

4.2 Computer simulations and results

Comparing with $LiNbO_3$ crystals, sillenite crystals are known as faster photorefractive crystals. It indicates that those crystals have larger carrier mobility μ and thermal generation rate β, which might conduct the unusual holographic experimental results in our Ru-doped BSO crystal with two trap centers. Thus, during numerical simulation, these two parameters are chosen to be much larger than those in $LiNbO_3$ crystals, as illustrated in Table 1. We first check experimental results shown in Figure 4 for the case of illumination with green gating and recording hologram simultaneously. Figure 6(a) shows the temporal evolution of the recording and read-out processes under different gating intensity. As it seen, the oscillation of the temporal response become larger in both recording and read-out stages as the intensity increases, which almost fits qualitatively with the observed experimental results. Since there are more than one unknown parameter, we do not attempt to fit the experimental curve quantitatively.

We then focus on the discussions about the influences of the thermal generation rates. Figure 6(b) shows the numerical results for cases with different thermal generation rates β_t and intensity of gating light at 800 mW/cm^2. As it seen, the thermal generation rate of deep trap β_t strongly influents the temporal evolution of the diffracted signal, meanwhile prolonged read-out process is detected as the thermal generation rate decreases. As a result, persistence of photorefractive hologram against erasure of the hologram by uniform read-out beam becomes saturated when β_t is small enough. It indicates that the key issue for achieving truly optical fixing in Ru-doped BSO is to grow the crystal with very low thermal generation rate. These analyses also indicate the holographic recording properties in Ru-doped BSO crystals can be tailored by introducing multiple trap center and excitation laser during the recording. However, more careful investigations of the influences of crystal parameters on the photorefractive grating are necessary in order to accomplish the desired response in practical applications.

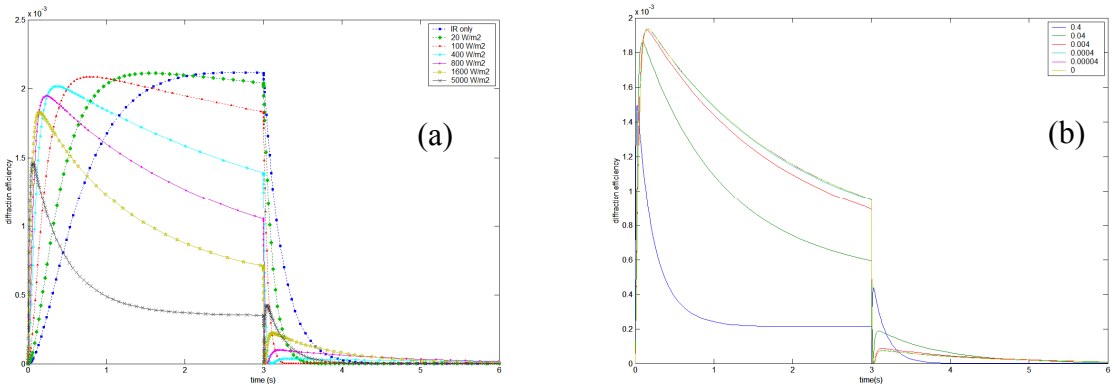

Figure 6. Temporal evolution of diffracted signal at both recording and read-out processes with (a). different intensity of gating laser during the recording (b) with different thermal generation rates β_t: the intensity of gating light is 800 mW/cm^2.

5. CONCLUSIONS

In summary, we have demonstrated that Ru addition in BSO crystal acts as very effective trap center, which improves the sensitivity and response speed at near infrared spectral range. Furthermore, an extended lifetime of hologram can be carried out by using 1064-nm writing beams and 532-nm green gating light simultaneously. These results show prospective features to use Ru-doped BSO for real-time holographic applications and image processing at near infrared spectral range, as well as for quasi-nondestructive read-out of photorefractive grating, which is particularly useful for bio-imaging application. Financial support by National Science Council, Taiwan under contracts # NSC 99-2911-1-009 -008 and NSC 97-2628-E-009-034-MY3 are gratefully acknowledged. Sample was grown by the Crystal Growth Laboratory of the Institute of Solid State Physics, Sofia.

References

[1] P. Gunter and J. -P. Huignard eds., *Photorefractive materials and their applications* 3 (Springer Berlin-Heilderberg, 2007).

[2] J. Frejlich, *Photorefractive materials* (Wiley Interscience, 2007).

[3] S. G. Odoulov, K. V. Shcherbin, and A. N. Shumeljuk "Photorefractive recording in BTO in the near infrared" JOSA B **11**, 1780-1785 (1994).

[4] P. V. dos Santos, J. Frejlich and J. F. Carvalho "Direct near infrared photorefractive recording and pre-exposure controlled hole-electron cometition with encahnced recording in undoped $Bi_{12}TiO_{20}$" Appl. Phys. B **81**, 651-655 (2005).

[5] E. Raita, O. Kobozev, A. A. Kamshilin and V. V. Prokofiev "Fast photorefractive response in $Bi_{12}SiO_{20}$ in the near infrared" Opt. Lett. **25**, 1261-1263 (2000).

[6] V Marinova, M. L. Hsieh , S. H. Lin, and K. Y. Hsu, "Effect of ruthenium doping on the optical and photorefractive properties of $Bi_{12}TiO_{20}$ single crystals" Opt. Comm. **203**, 377 -384 (2002).

[7] V. Marinova, S. H. Lin, V Sainov, M. Gospodinov, and K. Y. Hsu "Light-induced properties of Ru-doped $Bi_{12}TiO_{20}$ crystals" *J. Optics A: Pure and Applied Optics* **5**, S500- S506 (2003).

[8] F. Ramaz, L. Rakitina, M. Gospodinov and B. Briat, "Photorefrcative and photochromic properties of ruthenium –doped $Bi_{12}SiO_{20}$" Opt. Mat. **27**, 1547-1554 (2005)
[9] P. Sveshtarov and M. Gospodinov "The effect of the interface shape on authomatic Czochralski weight diameter control system performance" J. Crystal Growth **113**, 186-208 (1991).
[10] A. Delboulbe, C. Fromont, J. P. Herriau, S. Mallick and J.-P. Huignard "Quasi-nondestructive readout of holographically stored information in photorefractive $Bi_{12}SiO_{20}$ crystals" Appl. Phys Lett. **55**, 713-715 (1989).
[11] K. Buse, A. Adibi and D. Psaltis "Non-volatile holographic storage in doubly doped lithium niobate crystals" Nature **393**, 665-668 (1998).
[12] N.V.Kukhtarev, V.B. Markov, S.G. Odulov, M.S. Soskin and V. L. Vinetski "Holographic storage in electro-optic crystals I. Steady state" Ferroelectrics **22**, 949-960 (1979)

Table 1. The physical meanings and values of terms and parameters for theoretic modeling

Symbols	**Parameters**	**Values** [ ]
ε (F/m)	Dielectric constant	$56\varepsilon_0$
μ (m^2/Vs)	Carrier mobility	$2x10^{-6}$
T (K)	Temperature	300
e $(Coulomb)$	Electronic charge	$1.6x10^{-19}$
$I_{1,2}$ (W/m^3)	Optical intensity in the crystal	
I_{10} (W/m^3)	Optical intensity of excitation laser	up to 5000
I_{20} (W/m^3)	Optical intensity of writing laser	40000
K (μm^{-1})	Grating vector of interference pattern	6.11
N_A (m^{-3})	Density of acceptor	$1.0\ x10^{24}$
N_1 (m^{-3})	Density of deep traps	$1.9\ x10^{24}$
N_2 (m^{-3})	Density of shallow traps	$1.0\ x10^{24}$
N^+_1 (m^{-3})	Density of ionized deep traps	
N^+_2 (m^{-3})	Density of ionized shallow traps	
n (m^{-3})	Density of carrier in the conduction band	
$S_{11}(m^3/J)$	Photoionization cross section of deep trap at shorter wavelength	$1.2x10^{-4}$
$S_{21}(m^3/J)$	Photoionization cross section of shallow trap at shorter wavelength	$3.56x10^{-4}$
$S_{21}(m^3/J)$	Photoionization cross section of shallow trap at longer wavelength	$1.2x10^{-4}$
J (A/m^2)	Current density	
E (V/m)	Total electric field in the crystal	
$r_1(m^3/s)$	Carrier recombination rate constant of deep trap	$5.0x10^{-18}$
$r_2(m^3/s)$	Carrier recombination rate constant of shallow trap	$3.0x10^{-16}$
β_1 (s^{-1})	Thermal generation rate constant of deep trap	up to 0.4
β_2 (s^{-1})	Thermal generation rate constant of shallow trap	0.04
$\gamma(m/V)$	Electro-optical coefficient	$10.9x10^{-10}$
d (mm)	Thickness of crystal	1